

Journal of Mechanical Engineering

An International Journal

Volume 9 No. 1

July 2012

ISSN 1823-5514

Design Improvement of a Versatile Ducted-Fan UAV

Adnan Maqsood
Tiauw Hiong Go

Design and Flight Analysis of the Kenyalang-1 Fuel
Cell Powered Unmanned Aircraft

Thomas A. Ward

Effective Data Collection and Analysis for Efficient
Implementation of Standardized Work (SW)

Ahmed Jaffar
Nurul Hayati Abdul Halim
Noriah Yusoff

Knee Dynamic Analysis Based on 2D-to-3D Registration
of Fluoroscopic and Angiographic Images

Amir Hossein Savch
Ali Reza Zali
Seyyed Morteza Kazemi
Sohrab Keyhani
Hanafiah Yussof
Hamid Reza Katouzian
Qureish Vanat
Mahmoud Chizari

Longitudinal Static Stability of a Blended Wing-Body
Unmanned Aircraft with Canard as Longitudinal
Control Surface

Rizal E. M. Nasir
Wahyu Kuntjoro
Wirachman Wisnoe

Modal Extraction Accuracy Using Single Station Time
Domain (SSTD) Technique

A. F. Ghazali
A. A. Mat Isa

JOURNAL OF MECHANICAL ENGINEERING (JMeChE)

EDITORIAL BOARD

EDITOR IN CHIEF:

Professor Wahyu Kuntjoro – Universiti
Teknologi MARA, Malaysia

EDITORIAL BOARD:

Professor Ahmed Jaffar – Universiti Teknologi
MARA, Malaysia

Professor Bodo Heimann – Leibniz University
of Hannover Germany

Dr. Yongki Go Tiauw Hiong – Nanyang
Technological University, Singapore

Professor Mirosław L Wyszynski – University
of Birmingham, UK

Professor Ahmad Kamal Ariffin Mohd Ihsan –
UKM Malaysia

Professor P. N. Rao, University of Northern
Iowa, USA

Professor Abdul Rahman Omar – Universiti
Teknologi MARA, Malaysia

Professor Masahiro Ohka – Nagoya University,
Japan

Datuk Professor Ow Chee Sheng – Universiti
Teknologi MARA, Malaysia

Professor Yongtae Do – Daegu University,
Korea

Dr. Ahmad Azlan Mat Isa – Universiti
Teknologi MARA, Malaysia

Professor Ichsan S. Putra – Bandung Institute
of Technology, Indonesia

Dr. Salmiah Kasolang – Universiti Teknologi
MARA, Malaysia

Dr. Mohd. Afian Omar – SIRIM Malaysia
Dato' Professor Mohamed Dahalan Mohamed
Ramli – Universiti Teknologi MARA,
Malaysia

Professor Darius Gnanaraj Solomon – Karunya
University, India

Professor Mohamad Nor Berhan – Universiti
Teknologi MARA, Malaysia

Professor Bernd Schwarze – University of
Applied Science, Osnabrueck, Germany

Dr. Rahim Atan – Universiti Teknologi
MARA, Malaysia

Professor Wirachman Wisnoe – Universiti
Teknologi MARA, Malaysia

Dr. Thomas Ward – Universiti Teknologi
MARA, Malaysia

Dr. Faqir Gul – Institute Technology Brunei,
Brunei Darussalam

Dr. Valliyappan David a/l Natarajan –
Universiti Teknologi MARA, Malaysia

EDITORIAL EXECUTIVE:

Dr. Koay Mei Hyie
Rosnadiyah Bahsan
Farrashaida Mohd. Salleh
Mohamad Mazwan Mahat

© UiTM Press, UiTM 2012

All rights reserved. No part of this publication may be reproduced, copied, stored in any retrieval system or transmitted in any form or by any means; electronic, mechanical, photocopying, recording or otherwise; without prior permission in writing from the Director of UiTM Press, Universiti Teknologi MARA, 40450 Shah Alam, Selangor Darul Ehsan, Malaysia. e-mail: penerbit@salam.uitm.edu.my

Journal of Mechanical Engineering (ISSN 1823-5514) is published by the Faculty of Mechanical Engineering (FKM) and UiTM Press, Universiti Teknologi MARA, 40450 Shah Alam, Selangor, Malaysia.

The views, opinions and technical recommendations expressed herein are those of individual researchers and authors and do not necessarily reflect the views of the Faculty or the University.

Journal of Mechanical Engineering

An International Journal

Volume 9 No. 1

July 2012

ISSN 1823-5514

1. Design Improvement of a Versatile Ducted-Fan UAV 1
Adnan Maqsood
Tiauw Hiong Go
2. Design and Flight Analysis of the Kenyalang-1 Fuel Cell Powered Unmanned Aircraft 19
Thomas A. Ward
3. Effective Data Collection and Analysis for Efficient Implementation of Standardized Work (SW) 45
Ahmed Jaffar
Nurul Hayati Abdul Halim
Noriah Yusoff
4. Knee Dynamic Analysis Based on 2D-to-3D Registration of Fluoroscopic and Angiographic Images 79
Amir Hossein Saveh
Ali Reza Zali
Seyyed Morteza Kazemi
Sohrab Keyhani
Hanafiah Yusoff
Hamid Reza Katouzian
Qureish Vanat
Mahmoud Chizari

5. Longitudinal Static Stability of a Blended Wing-Body Unmanned Aircraft with Canard as Longitudinal Control Surface 99
Rizal E. M. Nasir
Wahyu Kuntjoro
Wirachman Wisnoe
6. Modal Extraction Accuracy Using Single Station Time Domain (SSTD) Technique 123
A. F. Ghazali
A. A. Mat Isa

Longitudinal Static Stability of a Blended Wing-Body Unmanned Aircraft with Canard as Longitudinal Control Surface

Rizal E. M. Nasir

Wahyu Kuntjoro

Wirachman Wisnoe

Flight Tech. & Test Centre

Faculty of Mechanical Engineering

Universiti Teknologi Mara, (UiTM) Shah Alam

ABSTRACT

Blended wing-body (BWB) aircraft, while having good aerodynamic efficiency, is hampered with issues related to its flight stability and control. To ensure longitudinal stability, a control canard is incorporated on Baseline-II E-2 BWB design. Mathematical representations of aerodynamic characteristics and stick-fixed trim flight stability, and analyses on the influence of some parameters to trim flight of this BWB aircraft with a control canard are highlighted and discussed. Baseline-II E-2 BWB aircraft is statically stable in longitudinal direction. However, this is true only for flight within low angles of attack. Mathematical models of trim flight parameters established here produces plots that have good agreement with plots of trim flight parameters found directly from wind tunnel experiments. Large static margin demands large positive canard angle for trim flight while agility can be achieved by moving the CG closer to aircraft's neutral point. The best static margin for Baseline-II E-2 BWB is chosen based on the best lift-to-drag ratio attainable during trim flight.

Keywords: *Flight Stability, Blended Wing-Body, Canard*

Nomenclature

| | |
|----------------------|---|
| α | Angle of attack (degree) |
| η_C or h_C | Canard deflection angle or canard setting angle (degree) |
| C_D | Drag coefficient |
| C_{D0} | Drag coefficient at zero lift or simply drag at zero lift |
| C_L | Lift coefficient |
| C_{L0} | Lift coefficient at zero angle of attack |
| C_M or C_{Mref} | Pitch moment coefficient at reference point usually aircraft's centre of gravity |
| C_{M0} | Pitch moment coefficient at zero lift |
| $C_{M(\alpha=0)}$ | Pitch moment coefficient at zero angle of attack |
| \bar{c} or MAC | Mean chord (metre) |
| CG | Centre of gravity |
| $dC_L/d\alpha$ | Change of lift coefficient with respect to change of angle of attack (per degree) |
| $dC_M/d\alpha$ | Change of moment coefficient with respect to change of angle of attack (per degree) |
| dC_M/dC_L | Change of moment coefficient with respect to change of lift. The negative of this parameter is known as static margin. Negative dC_M/dC_L indicates that the aircraft is statically stable. |
| h_{ref} or h | Centre of gravity location (reference point) in fraction of mean chord, MAC , from wing reference datum (the location where aircraft's mean chord begins) |
| k | Induced drag factor. $k = 1/(\pi e AR)$ where e is Oswald's efficiency coefficient and AR is aspect ratio of the aircraft's wing. |
| k' | Induced drag factor for cambered aircraft. Aircraft is said to be cambered if it has minimum drag at non-zero lift. A non-cambered aircraft has minimum drag at zero lift, which means that its drag at zero lift (C_{D0}) is also its minimum drag in drag polar plot. |
| K_η | Static margin – the distance of centre of gravity (reference point) to the neutral point is fraction of mean chord. Positive static margin means that the centre of gravity is located in front of neutral point indicating that the aircraft is statically stable. |
| L/D or dC_L/dC_D | Lift-to-drag ratio – usually associated with aerodynamic efficiency of an aircraft. |
| $(L/D)_{max}$ | Maximum lift-to-drag ratio |
| V | Airspeed |
| <i>trim</i> | This subscript denotes flight at trim condition (trim flight) where pitch moment is zero and the aircraft is at equilibrium (no acceleration, constant velocity) |

Introduction

Efficient flights can be achieved in various ways such as low-fuel consumption propulsion systems, lightweight materials and aerodynamic designs. One of the means of achieving good aerodynamic design is via introduction of blended wing-body (BWB) configuration. It is a 'hybrid' of flying wing and conventional fuselage-wing-tail types that has the advantages of having high-lift, low-drag aerodynamic characteristic of the former while also providing ample usable space for payload of the latter. Blended wing-body has a lifting body that is shaped like an airfoil. It is integrated to the wing onto the desired planform shape. Due to its lifting body, blended wing-body has larger amount of effective lifting area, increasing lift coefficient. Smooth transition of shape from the body to the wing reduces drag resulting increased lift-to-drag ratio which determines its flight efficiency during cruising mission [1]-[2].

Pitch moment is sensitive to change in lift, and also drag for some aircrafts. The lift and drag characteristic of some BWB aircrafts is slightly different than conventional wing-body-tail configuration aircraft. The lift curve (lift versus incidence angle) for conventional aircraft is often linear with some non-linearity near stall. This is not the case for BWB aircraft where the body itself creates significant amount of lift and continue to increase beyond wing stall angle that it may have negative impact on static stability of the whole aircraft as observed by Cummings et al. [3], Katz et al. [4] and Paul Pao et al. [5]. BWB's pitch moment coefficient-angle of attack plot is either unstable in terms of moment change w.r.t. angle of attack ($dC_M/d\alpha$)[6] or stable with reversal to unstable slope at mid. angles of attack [7].

Issues regarding flight stability and control being addressed include sizing of control surfaces, centre of gravity locations, airfoil shapes, wing-body incidence angles, wing sweep angle and planform shape. To take advantage of its full aerodynamic potential, blended wing-body aircraft is often designed as a tail-less aircraft, having all its control surfaces, usually elevons, on its wing and body. Tail-less blended wing-body aircraft, like flying wing, has issues with flight stability and control. Blended wing-body often has shorter body length compared to its wing span [8]. With its short pitch moment arm, changing its pitch attitude (such as angle of attack and pitch angle) requires large area of longitudinal control surfaces [5] or large control surface deflection angle. In other words, blended wing body aircraft demands large control power in longitudinal flight. Centre of gravity location for a blended wing-body is commonly near to its neutral point with some may have been placed behind the neutral point for easier pitch maneuverability. However, this may cause static and dynamic flight instability that requires full-time, sophisticated and expensive flight augmentation system [9]. Another problem of BWB aircraft is its tendency to tumble at certain flight condition [10]. Jung and Lowenberg recommend that

static margin for a flying wing should be small while initial pitch rate should be slow for a safe cruising flight [11].

Airfoil shape can be optimized to solve flight stability issues while improving lift-to-drag ratio. Airfoil sections along spanwise locations from centre of the body to wing tip can be customized to provide required forces and moments that are favorable for both flight efficiency and flight stability [12]-[13]. Incidence angles of these sections can also be tailored for the same reasons and one of the methods used is Inverse-Twist Method [12]. Sweep angle of the wing affects pitch moment characteristics that a study on it has been implemented on a blended wing-body design to seek the best angle that provides balance between longitudinal static stability and lift-to-drag ratio for specific flight conditions [14]. Similarly, planform shape can be designed, redesigned and optimized not only for flight stability and aerodynamic efficiency but also for structural design, flight performance, construction cost and other factors via various multi-disciplinary optimization (MDO) algorithms [15]-[16].

Bolsunovsky et al. envisaged various types of wing-body configurations such as blended wing-body, integrated wing-body, hybrid wing-body, and lifting-body that tailor to specific usage, performance requirements and flight missions [17]. Recommendations were highlighted on suitable longitudinal location of wing attached to body, body width and their effect to pitch moment. One of the recommendation is that the wing shall not be attached on the body's rearmost location otherwise serious nose-down moment may have occurred and poor pitch moment characteristic is found on BWB with body width larger than 22% overall wing span. There are blended wing-body designs that also incorporate separate control surfaces but they are limited to vertical tailplane.

UiTM's Blended Wing-Body Aircraft and Canard as Control Surface

To solve flight stability and control issues on small, unsophisticated, unmanned blended wing-body aircraft, a control canard is incorporated on Baseline-II BWB design. Baseline-II BWB is a part of Universiti Teknologi Mara's (UiTM) initiative to study the effect of canard to small blended wing-body in which its design is based on lessons learned from UiTM's Baseline-I BWB's poor aerodynamic and static stability characteristics [18]. Baseline-II BWB's aerodynamics has been studied via wind tunnel [19] and computational simulation method [20], and has been improved to E-1 and E-2 version with larger canard and modification to outer wing sections to increase lift-to-drag ratio while solving longitudinal static stability problems [21]. Canards, like elevators and elevons, is used mainly to change pitch moment and trim angle of attack that in effect can also alters aircraft's pitch angle, trajectory angles and airspeed. Canard is known to have inherent instability, mainly because its lift

creates pitch up moment that may cause tumbling of aircraft. Adding a canard to a wing-body moves neutral point forward and closer to centre of gravity, reducing static margin hence increasing $dC_M/d\alpha$ (from negative value to less negative value) resulting to large trim angle of attack change with small canard deflection angle change [22]. In other words, trim angle of attack change is relatively more sensitive to canard angle change than tailplane (elevator/elevon) angle change and this makes aircraft with canard more agile and maneuverable than conventional wing-tail aircraft. This extreme maneuverability costs reduction in stability, both static and dynamic, that in extreme condition, a wing-canard configuration is sometimes unstable.

Objective of Study

This paper focuses on Baseline-II E-2 BWB, shown in Figure 1, which is a 110-kg unmanned aerial vehicle of blended wing-body design fitted with canard that has a wing span of four metres and overall length of 2.37 metres. It is planned to be powered by a single turbojet engine or a unit of ducted fan driven either electric motor or internal combustion engine. In this paper, the mathematical representations of aerodynamic characteristics and stick-fixed trim flight stability, and analyses on the influence of some parameters to trim flight are highlighted and discussed.

Experiment Setup

Experiments have been carried out in UiTM LST-1 low speed wind tunnel with DARCS3D data acquisition giving 0.5% maximum error at full scale reading. The setup uses three-component external balance with 1:11 scale half model with 0.345 m span, 0.03995 m² wing-body plan form area, 0.114 m mean chord and moment reference centre (or centre of gravity) at 19.8% behind the leading edge of the mean aerodynamic chord, *MAC*. Aircraft's angle of attack in this case refers to incidence angle with respect to zero-lift line (so that $\alpha = 0$ at zero lift) of canard-less Baseline-II BWB aircraft model. The canard setting angle (η_c), like angle of attack, is measured with respect to zero-lift line of the said aircraft where, for both parameters, nose up attitude is taken as positive angle and vice-versa. Positive pitch moment causes pitch up attitude, positive lift refers to upward force and positive drag refers to rearward force with respect to wind axis. All experiments are conducted at average of 35 m/s airspeed (Mach 0.11) with average air density of 1.17 kg/m³ and average temperature of 24 degrees Celsius.

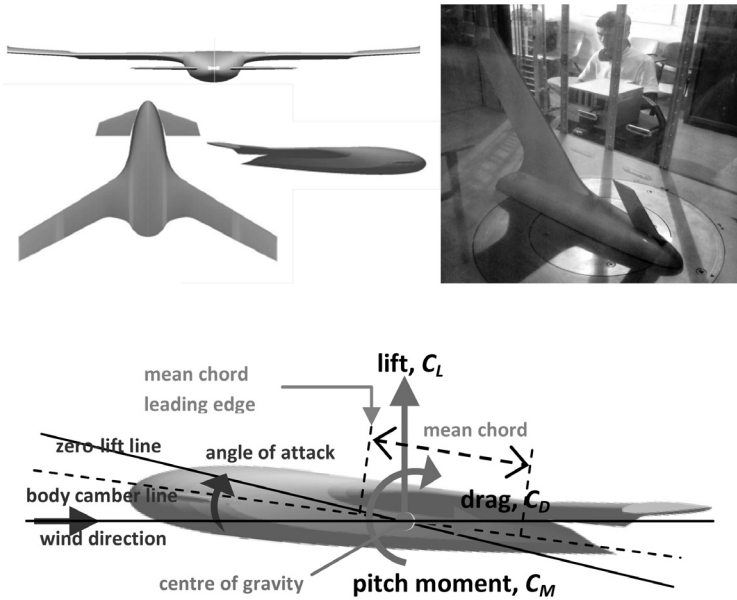
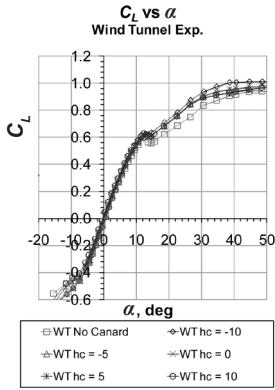


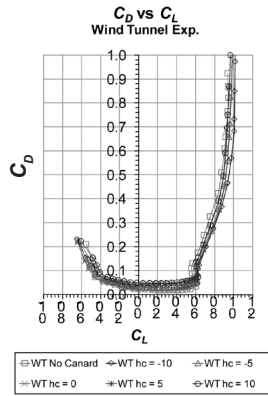
Figure 1: (a) Baseline-II E-2 Blended Wing-Body Three-view Pictures, (b) Its Wind Tunnel Model, and (c) Schematic Picture Showing Aerodynamic Forces, Moments and Other Important Parameters

Aerodynamic Characteristic at Low Angles of Attack

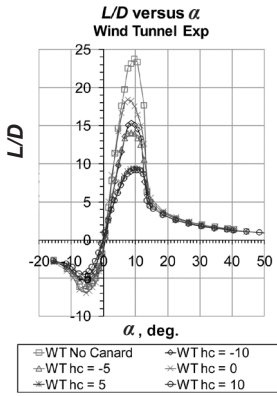
Figure 2 shows lift (C_L), drag (C_D), lift-to-drag ratio (L/D), and pitch moment at reference point (centre of gravity) (C_{Mref}) plots from wind tunnel experiments against angles of attack (α) and lift respectively. The reference point for pitch moment is located at 19.8% mean chord (MAC or c). It has been published and discussed in ref [21] that Baseline-II BWB's characteristics consist of low angles of attack region where the lift-angles of attack relationship is linear and the non-linear lift region. It is found that lift is linear within $0 \leq \alpha \leq 13$ degrees which corresponds to $0 \leq C_L \leq 0.6$. Pitch moment at reference centre plots also show almost similar linear patterns within the linear lift region while drag polar G_D vs G_L relationship is parabolic in nature. High lift-to-drag ratio (L/D) values are found within the region with maximum of almost 25 for without-canard case while installation of canard reduces L/D_{max} to mere 19 at canard setting angle $\eta_c = 0$ deg. Large absolute canard angle lowers the maximum lift-to-drag ratio attainable by Baseline-II BWB. Static stability behaviour of Baseline-II BWB that will be discussed later in this paper is limited to operational flight envelope within $0 \leq C_L \leq 0.6$.



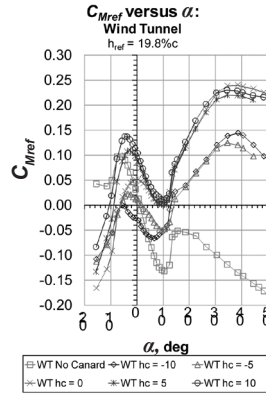
(a)



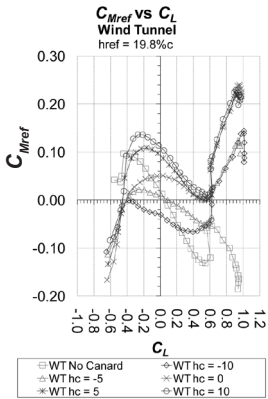
(b)



(c)



(d)



(e)

Figure 2: (a) C_L versus α (left), (b) C_D versus C_L (centre), (c) L/D versus α (right), (d) C_{Mref} versus α and (e) C_{Mref} versus C_L

Figure 3 shows lift-angle of attack (C_L vs α) and lift at zero angle of attack (C_{L0} vs η_c) plots within low angles of attack. If lift can be characterized by linear relationship, then;

$$C_L = \frac{dC_L}{d\alpha} \alpha + C_{L0} \tag{1}$$

where $dC_L/d\alpha$ is its lift slope in per degree. The $dC_L/d\alpha$ ranges from 0.056 to 0.060 for canard angle cases ranging from $-10 \leq \eta_c \leq +10$ deg. Assuming the slope changes little with respect to the change of η_c , the lift slope averages at;

$$\frac{dC_L}{d\alpha} = 0.0578 \text{ per deg.}$$

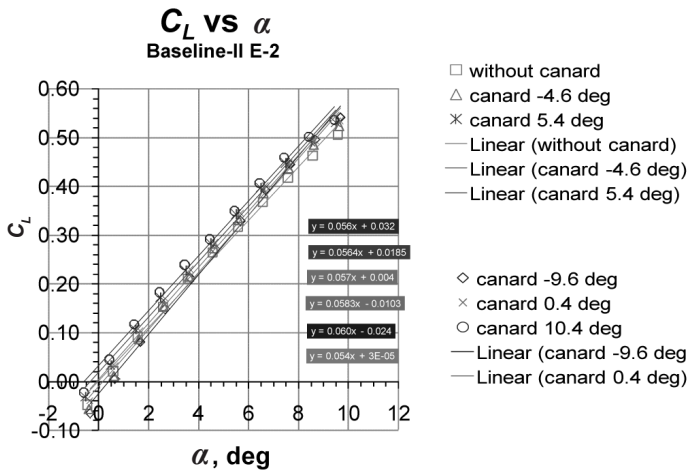


Figure 3: C_L versus α

Figure 3 enables one to find lift at zero angle of attack, C_{L0} , for each canard angle η_c case and relationship between the two is established in Figure 4. C_{L0} changes almost linearly with the change of η_c where;

$$C_{L0} = 0.00285 \eta_c + 0.00277 \tag{2}$$

Therefore, general lift-angle of attack-canard setting angle relationship can be summarized as;

$$C_L = 0.0578\alpha + 0.00285\eta_c + 0.00277 \tag{3}$$

Figure 5 shows C_D vs C_L and C_{D0} , k, k' vs η_c plots within low angles of attack. Drag (C_D) versus lift (C_L) plot can be characterized by parabolic relationship where;

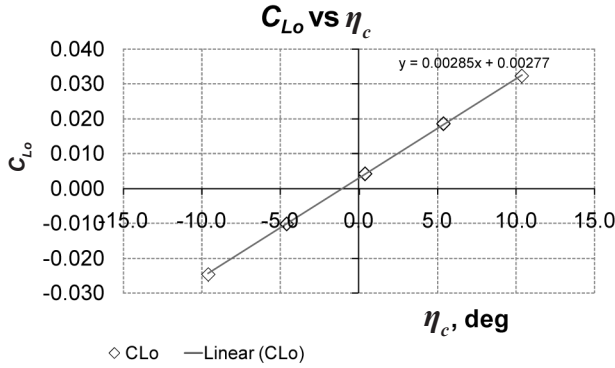


Figure 4: C_L versus α (left), C_{L0} versus η_c (right)

$$C_D = C_{D0} + k' C_L + k C_L^2 \tag{4}$$

Important parameters of drag are drag at zero lift (C_{D0}) and induced drag coefficients k' and k . The latter two depend on the value of lift. These parameters, plotted against canard setting angle η_c , are found to be;

$$C_{D0} = 0.000170\eta_c^2 + 0.00074\eta_c + 0.0218 \tag{5}$$

$$k' = 0.000023\eta_c^2 + 0.000156\eta_c + 0.0301 \tag{6}$$

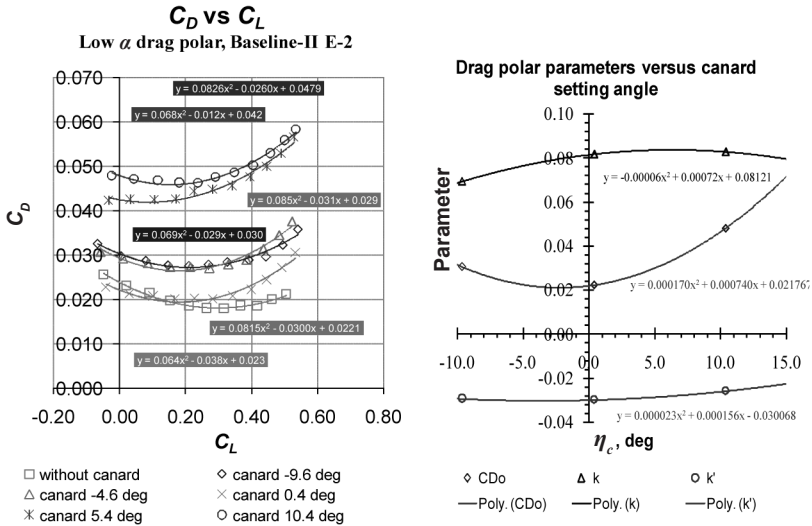


Figure 5: C_D versus C_L (left), C_{D0} , k and k' versus η_c (right)

$$k = 0.00006\eta_c^2 + 0.00072\eta_c + 0.0812 \quad (7)$$

Thus general drag-lift-canard angle relationship for Baseline-II BWB is;

$$C_D = (0.000170\eta_c^2 + 0.00074\eta_c + 0.0218) + (0.000023\eta_c^2 + 0.000156\eta_c + 0.0301)C_L + (0.00006\eta_c^2 + 0.00072\eta_c + 0.0812)C_L^2 \quad (8)$$

Based on Figure 6, moment at reference centre versus angle of attack relationship can be generalized as;

$$C_M = \frac{dC_M}{d\alpha} \alpha + C_M(\alpha=0) \quad (9)$$

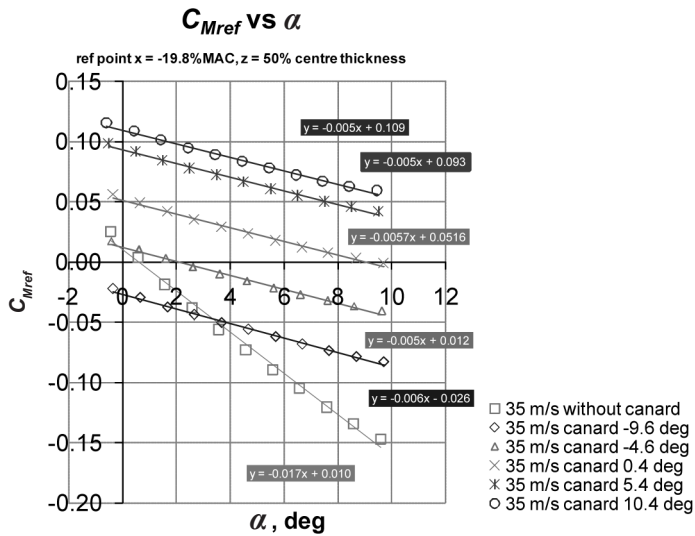


Figure 6: C_{Mref} versus α

where at reference point $h_{ref} = +0.198$ or 19.8% behind the wing datum, the average slope is calculated to be $\frac{dC_M}{d\alpha} = -0.0058$ per deg. Moment at zero angle of attack $C_{M(\alpha=0)}$ is plotted against η_c , as shown in Figure 7, and assuming that former changes linearly with changing canard angle then;

$$C_{M(\alpha=0)} = 0.00707\eta_c + 0.0451 \quad (10)$$

General moment-angle of attack-canard setting angle relationship is then summarized as;

$$C_M = -0.0058\alpha + 0.00707\eta_c + 0.0451 \quad (11)$$

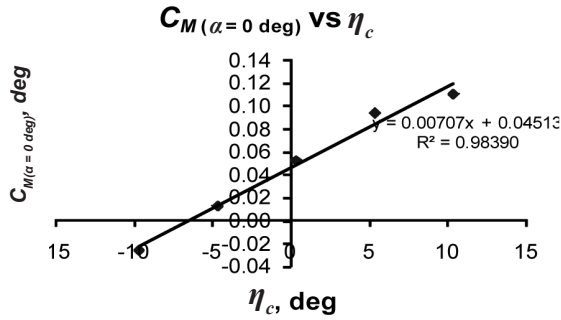


Figure 7: $C_{M(\alpha=0)}$ versus η_c

Following similar procedure and assumptions as C_{Mref} versus α plot, C_{Mref} versus C_L (Figure 8) general relationship can be determined based on;

$$C_M = \frac{dC_M}{dC_L} C_L + C_{M0} \tag{12}$$

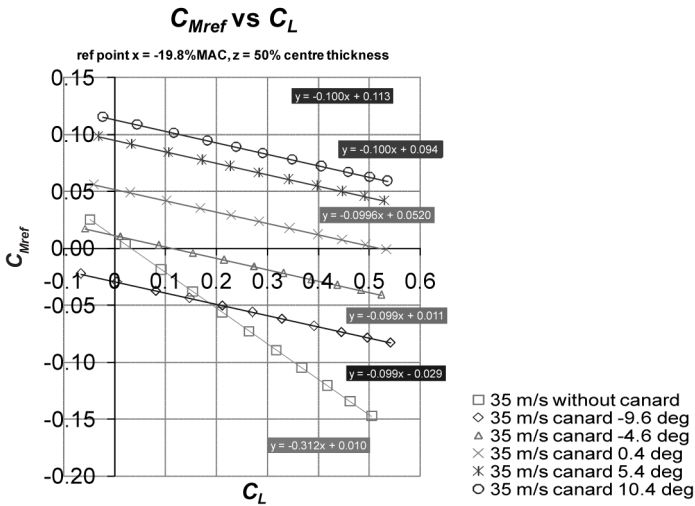


Figure 8: C_{Mref} versus C_L (left), C_{M0} versus η_c (right)

Average change of pitch moment coefficient with respect to change of lift coefficient is;

$$\frac{dC_M}{dC_L} = -K_n = -0.10$$

which indicates that the aircraft's static margin is around ten percent. Figure 9 shows pitch moment-at-zero lift C_{M0} versus canard angle η_c plot. Theoretically, C_{M0} changes linearly with changing η_c indicating the effect of canard on providing lift, hence increasing pitch moment, to the aircraft. However, Figure 9 suggests that the change $dC_{M0}/d\eta_c$ is not constant after $\eta_c > 10$ degree. If one assume that the relationship C_{M0} versus η_c is still linear then;

$$C_{M0} = 0.00735 \eta_c + 0.0454$$

Therefore, pitch moment versus lift relationship within linear region is;

$$C_M = -0.10C_L + 0.00735\eta_c + 0.0454 \quad (13)$$

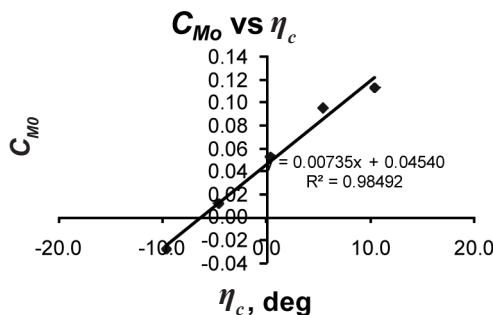


Figure 9: C_{Mref} versus C_L (left), C_{M0} versus η_c (right)

Positive value of static margin value indicates that the reference point is in front of aircraft's neutral point which is beneficial for its static stability. Increasing η_c increases trim lift (and also angle of attack), which is logical for canard-wing-body configuration.

Details on Trim Flight Condition: Establishing Mathematical Model

Trim flight is a condition where the moment at reference point is zero thus the aircraft is flying straight at a trim angle of attack. It is important to establish aerodynamic relationship for trim flight condition as a mean to compute the initial and final steady-state value when canard setting angle changed from one angle to another. Rewriting equations;

$$C_L = 0.0578\alpha + 0.00285\eta_c + 0.00277 \quad (14)$$

$$C_D = (0.000170\eta_c^2 + 0.00074\eta_c + 0.0218) + (0.000023\eta_c^2 + 0.000156\eta_c + 0.0301)C_L + (0.00006\eta_c^2 + 0.00072\eta_c + 0.0812)C_L^2 \quad (15)$$

$$C_M = -0.0058\alpha + 0.00707\eta_c + 0.0451 \quad (16)$$

$$C_M = -0.10C_L + 0.00735\eta_c + 0.0454 \quad (17)$$

If $C_M = 0$ (trim), then Equation (16) becomes;

$$\begin{aligned} C_{L(trim)} &= 0.0735\eta_{c(trim)} + 0.454 \\ \rightarrow \eta_{c(trim)} &= 13.61C_{L(trim)} - 6.176 \end{aligned} \quad (18)$$

Similarly at trim condition, Equation (17) becomes;

$$\begin{aligned} \alpha_{trim} &= 1.219\eta_{c(trim)} + 7.776 \\ \rightarrow \eta_{c(trim)} &= 0.818\alpha_{trim} - 6.386 \end{aligned} \quad (19)$$

Equation (19) is inserted into Equation (14) to find lift versus angle of attack relationship at trim flight condition;

$$\begin{aligned} C_{L(trim)} &= 0.0578\alpha_{trim} + 0.00285\eta_{c(trim)} + 0.00277 \\ C_{L(trim)} &= 0.0578\alpha_{trim} + 0.00285(13.61C_{L(trim)} - 6.176) + 0.00277 \\ C_{L(trim)} &= 0.0612\alpha_{trim} - 0.0154 \end{aligned} \quad (20)$$

Meanwhile, Equation (18) is inserted into Equation (15) for drag versus lift relationship at trim flight condition;

$$\begin{aligned} C_{D(trim)} &= (0.000170[13.61C_{L(trim)} - 6.176]^2 + 0.00074[13.61C_{L(trim)} \\ &\quad - 6.176] + 0.0218) \\ &\quad + (0.000023[13.61C_{L(trim)} - 6.176]^2 \\ &\quad + 0.000156[13.61C_{L(trim)} - 6.176] + 0.0301)C_{L(trim)} \\ &\quad + (0.00006[13.61C_{L(trim)} - 6.176]^2 \\ &\quad + 0.00072[13.61C_{L(trim)} - 6.176] + 0.0812)C_{L(trim)}^2 \end{aligned}$$

Neglecting $C_{L(trim)}^4$ and $C_{L(trim)}^3$ (too small);

$$C_{D(trim)} = 0.0234 - 0.0468C_{L(trim)} + 0.111C_{L(trim)}^2 \quad (21)$$

Similar approach can be found for drag versus canard angle relationship at trim flight condition ($C_{D(trim)} - \eta_{c(trim)}$);

$$C_{D(trim)} = 0.0251 + 0.004\eta_{c(trim)} + 0.0006\eta_{c(trim)}^2 \quad (22)$$

Lift-to-drag ratio versus canard angle for trim flight is derived from combination of Equations (18) and (22);

$$\left(\frac{C_L}{C_D}\right)_{trim} = \frac{C_{L(trim)}}{C_{D(trim)}} = \frac{0.0735\eta_{c(trim)} + 0.454}{0.0251 + 0.004\eta_{c(trim)} + 0.0006\eta_{c(trim)}^2} \quad (23)$$

Equations (18) until (23) become mathematical representation (model) of aerodynamics and flight stability of Baseline-II E-2 BWB aircraft at trim condition. This will later be used to calculate flight dynamic coefficients and derivatives. To ensure validity of these model equations, comparisons are made with trim data found directly from wind tunnel experiment and plotted in Figures 10 until 15. The solid lines (legend: \diamond -model) are the plots calculated from mathematical relationship established in equations 18-23. The dotted lines (legend: Δ -exp) with triangular points are plots of parameters at trim conditions found directly from wind tunnel experiment plots in Figure 2 in the early part of this paper.

The mathematical model plots differ only slightly to the plots from the experiment, and the differences are noticeable at angles of attack larger than 10 degrees. These differences are due to 1) linearization of C_L versus α relationship where as dC_L/α (lift-angle of attack slope) reduces slightly as angle of attack

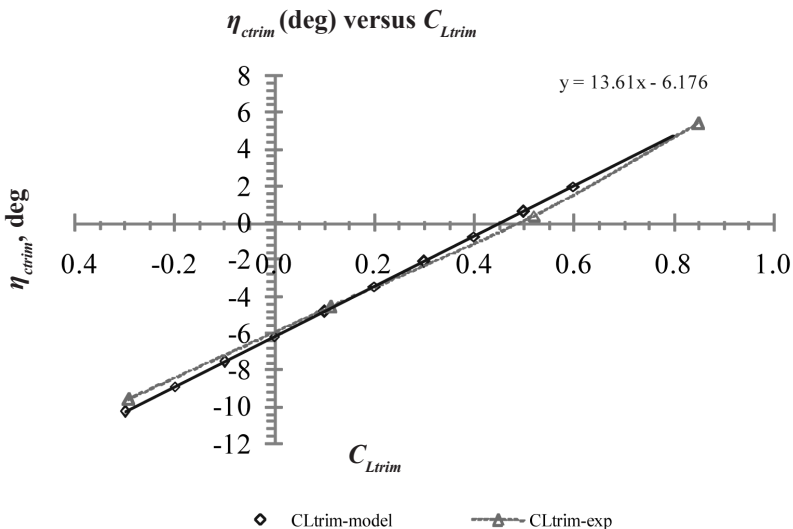


Figure 10: $\eta_{c(trim)}$ versus $C_{L(trim)}$ - Equation (18)

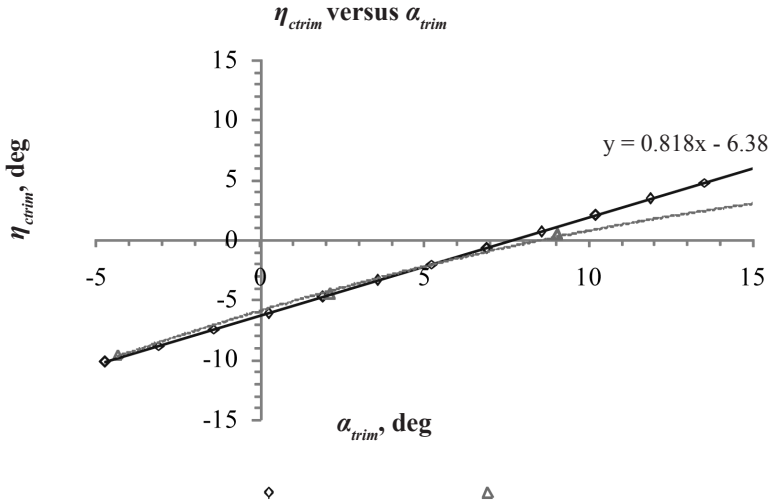


Figure 11: $\eta_{c(trim)}$ versus α_{trim} - Equation (19)

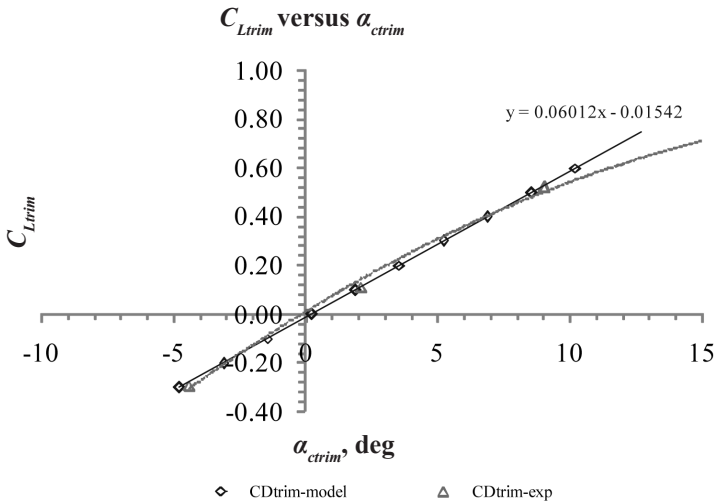


Figure 12: $C_{L(trim)}$ versus α_{trim} - Equation (20)

increases, 2) reduction of order for $C_{D(trim)}$ versus $C_{L(trim)}$ relationship from four to two (C_L^4 and C_L^3 are neglected), and 3) rounding off error. In short, the mathematical model of Baseline-II BWB presented here can be accepted as representation of its aerodynamic behavior for normal cruising flight condition

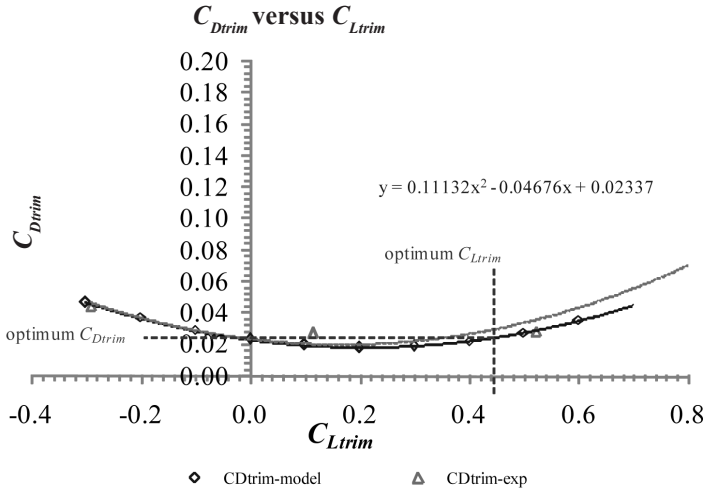


Figure 13: $C_{D(trim)}$ versus $C_{L(trim)}$ - Equation (21)

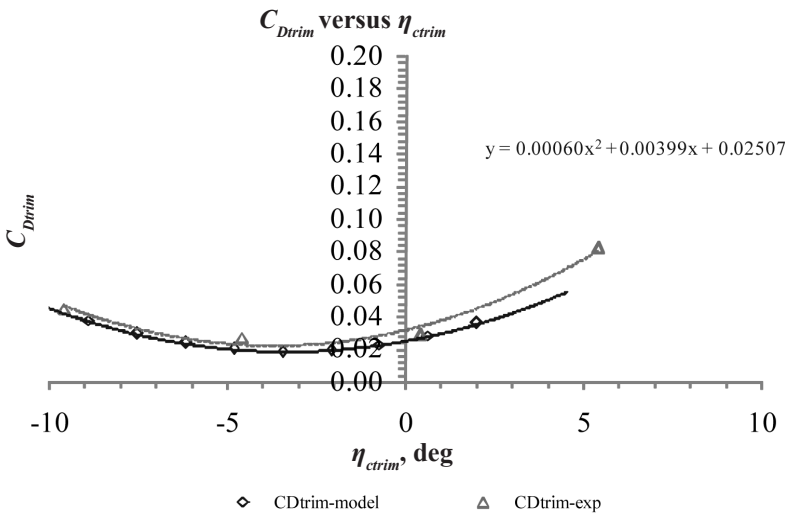


Figure 14: $C_{D(trim)}$ versus $\eta_{c(trim)}$ - Equation (22)

where trim angle of attack does not exceed 10 degrees. $(C_L/C_D)_{trim} - \eta_c$ plot shows that maximum lift-to-drag ratio can be found at η_c slightly below 0.0° . This corresponds to, if we look at Figures 10, 11 and 14, $C_{L(trim)} \cong 0.45$, $\alpha_{trim} \cong 7.5^\circ$ and $C_{D(trim)} \cong 0.022$ giving maximum lift-to-drag ratio of 18.2. This will be the optimum flight condition for cruising.

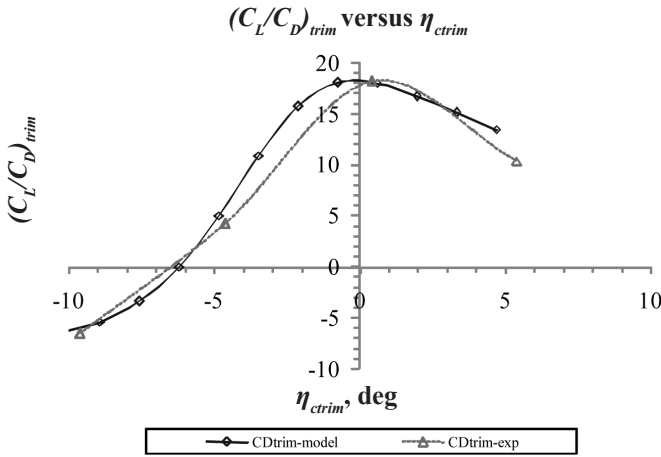


Figure 15: $(C_L/C_D)_{trim}$ versus $\eta_{c(trim)}$ - Equation (23)

The Effect of Centre of Gravity to Longitudinal Static Stability

The study is extended to the effect of centre of gravity (CG) locations to stick-fixed trim flight stability. Baseline-II BWB's canard control is of powered-type (electric motor-actuator) thus stick-free stability study is deemed unnecessary. Plots in Figures 16 to 19 show the effect of CG to canard angle to trim lift $C_{L(trim)}$, cruising speed V_{trim} , angle of attack α_{trim} and canard sensitivity

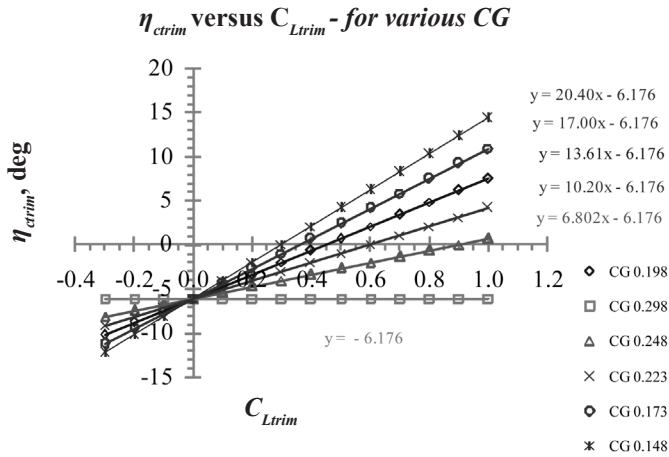


Figure 16: $\eta_{c(trim)}$ versus $C_{L(trim)}$ for various CG ($h = 0.148 - 0.298$)

$d\eta_{c(trim)}/dC_{L(trim)}$. Six CG locations are highlighted here where all aerodynamic coefficients are computed using equations mentioned before. These CG locations ranges from $h = 14.8\% \bar{c}$ to $h = 29.8\% \bar{c}$ (\bar{c} is mean chord of the wing-body) which equals to static margin from $K_n = +15.0\% \bar{c}$ to $K_n = +0.0\% \bar{c}$.

Figure 16 shows that large static margin, which equals to the large distance of CG in front of the neutral point, has high $d\eta_{c(trim)}/dC_{L(trim)}$ meaning that large canard deflection angle is needed for a unit trim lift. If one sets Baseline-II BWB's CG forward at $h = 14.8\% \bar{c}$ ($K_n = +15.0\% \bar{c}$) and wants to trim at cruising lift of $C_{L(trim)} = 0.45$, the canard setting needed is about $K_n = +4.0^\circ$ while setting the CG very near to the neutral point such as at $h = 24.8\% \bar{c}$ ($K_n = +5.0\% \bar{c}$) will require canard setting to be $\eta_c = -3.0^\circ$. There is no problem for locating CG at these two locations but the lift-to-drag ratio for cruising at $C_{L(trim)} = 0.45$ reduces to around 13.0-14.0 (Figure 15). Both of these are not as efficient as putting the CG at $h = 19.8\% \bar{c}$ ($K_n = +10.0\% \bar{c}$) that requires canard setting angle to be $\eta_c = -0.0^\circ$ with lift-to-drag ratio of 18.2.

The change of CG location, h , changes the slope of $\eta_c - C_{L(trim)}$ plots known as canard sensitivity to lift, $d\eta_{c(trim)}/dC_{L(trim)}$. The further back the location of CG, or the closer the CG to the neutral point (as long as CG is in front of the neutral point) the lower the slope, meaning that less canard angle is needed to change the lift. This makes the Baseline-II BWB flight movement more sensitive to canard angle changes thus making it more maneuverable. However, high maneuverability has unfavorable effect to the stability of the flight especially when one decides not to implement complex and expensive electronic flight control system. Relocating the CG further back to the neutral point ($h = 29.8\% \bar{c}$ or $K_n = +0.0\% \bar{c}$) causes Baseline-II BWB to be neutrally stable and trim flight will not be possible.

The effect of centre of gravity location h and static margin K_n to canard sensitivity to lift is shown in Figure 17. The sensitivity of canard to lift studied

here ranges from $\frac{d\eta_c}{dC_{L(trim)}} = 20.4^\circ$ per unit lift for $h = 14.8\% \bar{c}$ ($K_n = +15.0\% \bar{c}$)

to $\frac{d\eta_c}{dC_{L(trim)}} = 6.8^\circ$ per unit lift for $h = 24.8\% \bar{c}$ ($K_n = +5.0\% \bar{c}$). The former

case means that Baseline-II BWB is highly stable and may need large control power (larger, more powerful motor-actuator) for a small change of trim attitude while the latter has the opposite effect where it may have 'light steering feel'. Sensitivity for CG location at neutral point is zero.

The effect of CG location to trim angle of attack, as highlighted in Figure 18, is similar to trim lift as both are linked by a linear relationship. In other words, the closer the CG to the neutral point the more sensitive the canard has become; just a small canard change is needed to change a unit of angle of attack. For the two extreme cases highlighted here, the sensitivity of canard to angle of attack $d\eta_c/d\alpha$ is 1.25 for $h = 14.8\% \bar{c}$ ($K_n = +15.0\% \bar{c}$) and $d\eta_c/d\alpha$ is 0.40 for

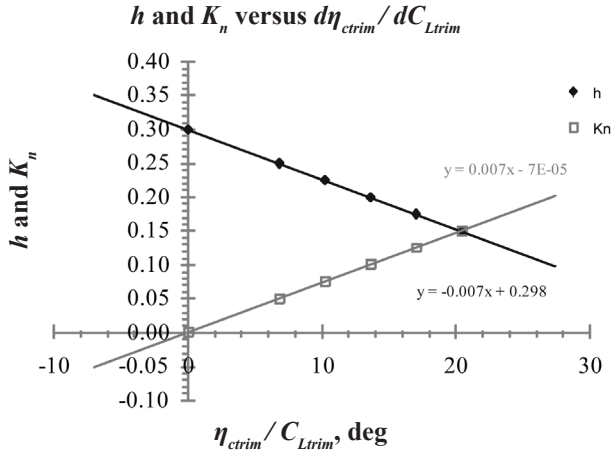


Figure 17: CG Location and Static Margin Versus Canard Sensitivity to Lift

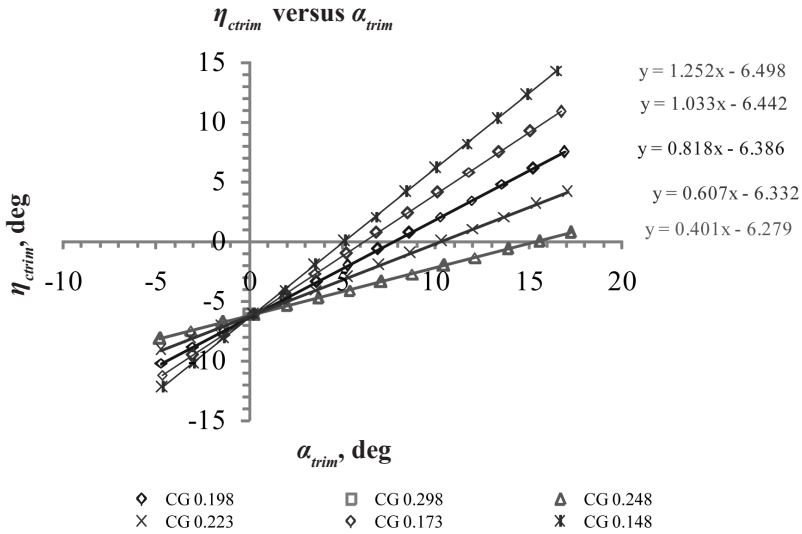


Figure 18: $\eta_{c(trim)}$ versus α_{trim} for various CG ($h = 0.148 - 0.298$)

$h = 24.8\% \bar{c}$ ($K_n = +5.0\% \bar{c}$). Just like sensitivity to lift, $d\eta_c/d\alpha$ is 0.00 for CG at neutral point.

Angle of attack, lift, drag and CG location affect cruising airspeed. Figure 19 shows canard angle versus airspeed at trim flight condition for various CG locations. This figure enables one to predict canard angle needed to fly steady

and level at any given airspeed and CG location within its operating limit. Trim airspeed is computed based on;

$$V_{trim} = \sqrt{\frac{m_{aircraft}g}{0.5\rho S(C_L)_{trim}}} \tag{24}$$

where $m_{aircraft}$, g , ρ and S are aircraft’s weight, air density and reference wing-body area respectively. As mentioned the mass of Baseline-II BWB is 110 kg. For this analysis, air density is taken at 1.225 kg/m³ which is sea level value based on International Standard Atmosphere (ISA). Trim airspeed now can be expressed as equivalent airspeed V_{EAS} .

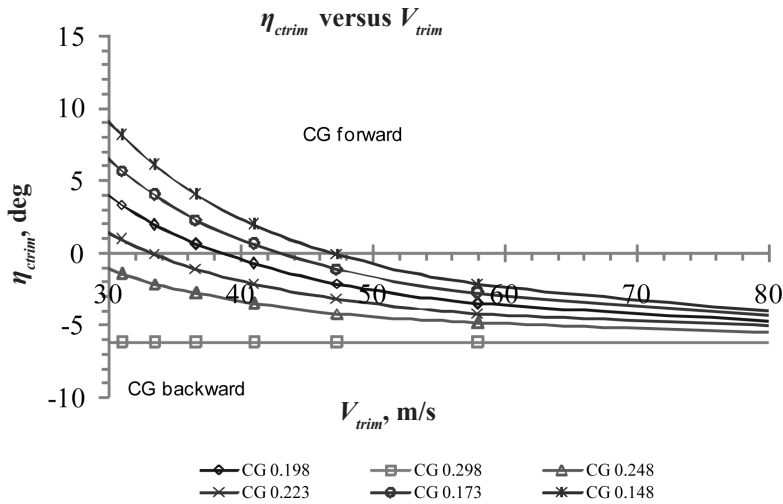


Figure 19: $\eta_{c(trim)}$ versus V_{trim} for various CG ($h = 0.148 - 0.298$)

For maximum L/D of 18.2, one must fly at equivalent airspeed $V_{EAS} = 43.0$ m/s (154.8 km/h) with $\eta_c = 0.0^\circ$ for CG at $h = 19.8\% \bar{c}$ ($K_n = +10.0\% \bar{c}$). Moving the CG forward, for example to $h = 14.8\% \bar{c}$ ($K_n = +15.0\% \bar{c}$) while maintaining canard setting angle of $\eta_c = 0.0^\circ$, causes trim airspeed to increase to $V_{EAS} = 47.5$ m/s (171.0 km/h) because at this CG location and canard angle, $C_{L(trim)} \cong 0.30$ and $\alpha_{trim} = 5.0^\circ$. Now that the angle of attack and lift has changed, the lift-to-drag ratio is also expected to change to just mere 15.0. Moving the CG backward to $h = 24.8\% \bar{c}$ ($K_n = +5.0\% \bar{c}$) while maintaining $\eta_c = 0.0^\circ$ causes airspeed to decrease too much (less than 30.0 m/s) that its lift and angle of attack increases to $C_{L(trim)} \cong 0.90$ and $\alpha_{trim} \cong 15.0^\circ$. If refer to Figure 2 earlier, then one may or may not know the possibility of trim flight at this angle of attack and lift as it

lies into the non-linear lift-angle of attack region that is out of the scope of this paper. It should be noted that the study here is limited to maximum lift of $C_L = 0.6$. However, having the CG at $h = 24.8\% \bar{c}$ ($K_n = +5.0\% \bar{c}$) does not mean that Baseline-II BWB cannot trim its flight; it can, in fact, but with canard setting angle less than -30° .

Concluding Remarks

Baseline-II E-2 BWB aircraft is statically stable in longitudinal direction. However, this is true only for flight within low angles of attack ranging within $0 \leq \alpha \leq +13$ degrees which corresponds to $0 \leq C_L \leq 0.6$. Stability reversal, where the stability of an aircraft changes from stable to unstable, is observed at angles of attack beyond linear-lift region. Mathematical models of trim flight parameters established here produces plots that have good agreement with plots of trim flight parameters found directly from wind tunnel experiments. Significant differences between the mathematical models and wind tunnel experiments results are observed for trim flight parameters at angles of attack larger than 10 degrees (but still not exceeding 13 degrees) due to some possible factors aforementioned. Large static margin demands large positive canard angle for trim flight and vice-versa. Agility can be achieved by moving the CG closer to aircraft's neutral point, in other words, reducing static margin. Further reduction of static margin causes instability that can only be overcome by sophisticated electronic flight control algorithm. Static margin of 10.0 percent is chosen for Baseline-II E-2 case because it requires canard setting angle of 0.0 degree to trim at the highest possible lift-to-drag ratio. This is so far the best static margin for Baseline-II E-2 BWB.

Acknowledgements

Authors would like to express gratitude to the Ministry of Higher Education Malaysia (MoHE), Faculty of Mechanical Engineering, and Research Management Institute, Universiti Teknologi MARA for funding the research under Fundamental Research Grant Scheme (FRGS) and Dana Kecemerlangan Pasca-Siswazah (600-RMI/ST/DANA 5/3/Dst (219/2009) funds.

References

- [1] R.M. Cummings, S.A. Morton and S.G. Siegel (2008). *Numerical prediction and wind tunnel experiment for a pitching unmanned combat air vehicle*. Aerospace Science and Technology 12, 355-364.

- [2] J. Katz, S. Byre and R. Hahl (1999). *Stall resistance features of lifting body airplane configurations*. Journal of aircraft 36(2), 471-478.
- [3] N. Qin, A. Vavalle, A. Le Moigne, M. Laban, K. Hackett and P. Weinnerfelt (2002). *Aerodynamic Studies for blended wing body aircraft*. AIAA 2002-5448 9th AIAA/ISSMO Symposium on Multidisciplinary Analysis and Optimization, 4-6 September 2002, Atlanta, Georgia, 1-11.
- [4] A. Bergmann and D. Hummel (2001). *Aerodynamic Effects of Canard Position on a Wing Body Configuration in Symmetrical Flow*. AIAA-2001-0116, 39th AIAA Aerospace Sciences Meeting & Exhibit, 8-11 Jan. 2001, Reno, Nevada.
- [5] Y.D. Staelens, R.F. Blackwelder and M.A. Page (2008). *Computer simulation of landing, take off and go-around of a blended-wing-body airplane with belly flaps*. AIAA 2008-297, 46th AIAA Aerospace Sciences Meeting and Exhibit. 7-10 January 2008, Renon, Nevada.
- [6] H.V. de Castro (2003). *Flying and handling qualities of a fly-by-wire blended-wing-body civil transport aircraft*. PhD. Thesis. Cranfield University.
- [7] S. Saephan and C.P. Van Dam (2003). *Simulation of the tumbling behaviour of tailless aircraft*. AIAA 2006-3321, 24th Applied Aerodynamics Conference, 5-8 June 2008, San Francissco, California (2008).
- [8] D.W. Jung and M.H. Lowenberg. *Stability and control assessment of a blended-wing-body airliner configuration*. AIAA Atmospheric Flight Mechanics Conference and Exhibition, 15-18 August 2005, San Francisco, California (2005).
- [9] N. Qin, A. Vavalle, A. Le Moigne, M. Laban, K. Hackett and P. Weinnerfelt (2004). *Aerodynamic considerations of blended wing body aircraft*. Progress in Aerospace Science 6, 321-343.
- [10] S. Wakayama and I. Kroo (2000). *The Challenge and Promise of Blended-Wing-Body Optimization*. AIAA Technical Paper 2000-4740.
- [11] S. Siouris, N. Qin (2007). *Study of the effects of wing sweep on the aerodynamic performance of a blended wing body aircraft*. Proceedings of Inst. of Mech. Engineers. Vol. 221. Part G: Journal of Aerospace Engineering, 47-55.

- [12] H. Engels, W. Becker and A. Morris (2004). *Implementation of a multi-level methodology within the e-design of a blended wing body*. Aerospace Science and Technology 8, 145-153.
- [13] C. Österheld, W. Heinze and P. Horst (2004). *Preliminary Design of A Blended Wing Body Configuration Using The Design Tool PrADO*. Aerospace Science and Technology 8, 154-168.
- [14] L. Bolsunovsky, N. P. Buzoverya, B. I. Gurcvich, V. E. Denisov, A. I. Dunacvsky, L. M. Shkadov, O. V. Sonin, A. J. Udzhuhu and J. P. Zhurihin (2001). *Flying Wing-Problems and Decisions*. Aircraft Design 4, 193-219.
- [15] Rizal E. M. Nasir, Wahyu Kuntjoro, Wirachman Wisnoe, Zurriati Ali, Nor F. Reduan, Firdaus Mohamad and Shahrizal Suboh (2010). *Preliminary Design of "Baseline-II" Blended Wing-Body (BWB) Unmanned Aerial Vehicle (UAV): Achieving Higher Aerodynamic Efficiency Through Planform Redesign and Low-Fidelity Inverse Twist Method*. Proceedings of 3rd Engineering Conference on Advancement in Mechanical and Manufacturing for Sustainable Environment (EnCon2010), April 14-16 2010, Kuching, Sarawak.
- [16] Wirachman Wisnoe, Wahyu Kuntjoro, Firdaus Mohamad, Rizal Effendy Mohd Nasir, Nor F. Reduan and Zurriati Ali (2010). *Experimental Results Analysis for UiTM BWB Baseline-I and Baseline-II UAV Running at 0.1 Mach number*. International Journal of Mechanics 4(2), 23-32.
- [17] Rizal E. M. Nasir, Wahyu Kuntjoro, Wirachman Wisnoe, Zurriati Mohd. Ali, Norfazira Reduan, Firdaus Mohamad and Ramzyzan Ramly (2010). *Static Stability of Baseline-II Blended Wing-Body Aircraft at Low Subsonic Speed: Investigation via Computational Fluid Dynamics Simulation*. 2010 International Conference on Science and Social Research (CSSR 2010), December 5-7, 2010, Kuala Lumpur, Malaysia.
- [18] Rizal E. M. Nasir, Wahyu Kuntjoro, Wirachman Wisnoe, Zurriati Ali, Norfazira Reduan, Firdaus Mohamad and Ramzyzan Ramly (2010). *Aerodynamics and Longitudinal Static Stability of Baseline-II Blended Wing-Body Aircraft Variants*. 2010 International Conference on Advances in Mechanical Engineering (ICAME 2010), December 2-5, 2010, Shah Alam, Malaysia.
- [19] M.V. Cook (2007). *Flight Dynamics Principle, 2nd ed.*, Elsevier, Amsterdam.